Quantifying Supercritical CO_2 Dilation of Poly(vinylidene fluoride) and Poly(vinylidene fluoride-*co*-hexafluoropropylene) Utilizing a Linear Variable Differential Transducer: Plasticization and Melting Behavior

*Suresh L. Shenoy, Tomoko Fujiwara, Kenneth J. Wynne**

Chemical Engineering Department, School of Engineering, Virginia Commonwealth University, 601 West Main St., Richmond, VA 23284-3028, USA

Summary: Melting behavior of semicrystalline poly(vinylidene fluoride) (PVDF) and poly(vinylidene fluoride-*co*-hexafluoropropylene) is investigated as a function of supercritical CO_2 pressure using a Linear Variable Displacement Transformer (LVDT). The melting temperature (T_m) of both polymers is lowered due to supercritical CO_2 plasticization. For PVDF, the maximum lowering of T_m (ΔT_m=23°C) occurs between 483 and 552 bar. The corresponding value for the copolymer is ΔT_m = 26°C at 552 bar. At higher pressures, hydrostatic effects override plasticization and T_m increases for both polymers. By comparing T_m in N_2, a noninteracting gas, the opposing effects of plasticization and hydrostatic pressure on T_m are explored.

Keywords: LVDT, melting point, PVDF, supercritical CO_2, swelling

Introduction

Polymer plasticization by high-pressure carbon dioxide has been investigated by obtaining sorption isotherms,[1-3] measuring polymer dilation,[1,4-6] and by depression of glass transition temperatures (T_g).[7-10] A vast majority of these studies have focused on amorphous polymers.[1,4,5,7,8,11,12] The behavior of semicrystalline polymers in high pressure CO_2 is more complex.[2,10,13-23] In semicrystalline polymers, plasticization of strained amorphous regions adjacent to crystalline lamellae, can result in CO_2-induced crystallinity or "anti-plasticization".[13-16] For example, plasticization and anti-plasticization of poly(ethylene terephthalate) (PET)[13,15,16] and polycarbonate (PC)[14,24] in high pressure CO_2 have been extensively studied. The effect of CO_2 on other semicrystalline polymers such as low density polyethylene (LDPE),[17] polytetrafluoroethylene (PTFE),[19] poly(vinylidene fluoride)[2] (PVDF) and polyurethanes[18] has also been studied at relatively low temperatures.

Recently we developed a method that utilizes a Linear Variable Differential Transformer (LVDT) to quantify plasticization of polymers. The versatility and robustness of this technique permit in situ measurements at high temperatures and pressures. Using this method

 DOI: 10.1002/masy.200351120

we reported swelling behavior in $SCCO_2$ of styrene-butadiene-styrene triblock copolymer (elastomer)[25] and PVDF (semicrystalline).[26]

To employ supercritical CO_2 as a processing aid for semicrystalline polymers information about melting behavior as a function of pressure is desirable. The melting temperature (T_m) is defined as the temperature at which the chemical potentials of amorphous and crystalline phases are equal ($\Delta\mu_a = \Delta\mu_{cry}$). The chemical potential of the amorphous regions decreases due to polymer-CO_2 interactions. As a result, T_m decreases. For example, at 77 bar in supercritical CO_2 the T_m of syndiotactic PS (270°C) decreases by about 12°C.[27]

In addition to quantifying plasticization, the LVDT technique can be utilized to monitor the effect of supercritical CO_2 on T_m as a function of pressure. The lowering of PVDF homopolymer T_m in supercritical CO_2 was previously examined.[26] In this paper we compare and contrast the melting behavior of PVDF homopolymer and a PVDF copolymer containing 4.9 mol% hexafluoropropylene (HFP) comonomer units.

Experimental

Materials. Liquid CO_2 (bone dry) was obtained from Roberts Oxygen Company, Inc. Poly(vinylidene fluoride), [Catalog #102, M_w=530,000 and T_m =158°C], was obtained from Scientific Polymer Products, Inc. and was used as received. PVDF powder was melt pressed in a Carver Laboratory Press at 230°C for 20 minutes followed by fast cooling to room temperature. The PVDF-copolymer containing 4.9 mol% hexafluoropropylene (PVDF-HFP) [M_w=290,000 and T_m =138.9°C] was supplied in the form of 4.7 mm OD x 3.2 mm ID tubing by Daikin America Technical Center. For PVDF T_m measurements, rectangular bars (≈1 cm x 0.35 cm x 0.2 cm) were cut from melt pressed discs with a small saw and sanded to regular dimensions. For PVDF-copolymer, tubing sample (1cm length) was cut using a razor.

Equipment. Differential scanning calorimetry (DSC) measurements were carried out using a Perkin Elmer DSC Pyris-1. Details of the experimental setup have been described in a previous paper. [25]

Measurements. Calibration, sample setting, and data acquisition were performed as previously reported.[25] Dilation is reported as percent change in the sample length $(\Delta L/L_o)x100\%$, where $\Delta L = L_t - L_o$, L_t is the length of the sample at time t, and L_o is the initial sample length.

To measure T_m, supercritical CO_2 pressure was increased to the desired value at a temperature below T_m. LVDT readings were noted at regular intervals. When the sample attained maximum swelling, the LVDT readings remained constant for 20-30 minutes. The temperature was then increased by 3-4°C incrementally, while employing the manual pressure generator to maintain constant $SCCO_2$ pressure during temperature increase. The dilation includes thermal expansion as well as swelling due to CO_2. At the melting temperature T_m, $\Delta L/L_o$ decreased markedly due to sample softening and the experiment was terminated.

Results and Discussion

Thermal analyses of melt pressed PVDF and as received PVDF-copolymer were performed by DSC (data not shown). For PVDF homopolymer, the maximum in melting peak occurs at 158.0°C. The corresponding maximum in the melting endotherm for the copolymer appears at 138.9°C. The lower T_m reflects presence of more imperfect crystallites due to the bulky hexafluoropropylene comonomer.

PVDF homopolymer. Figure 1 shows a representative plot of $\Delta L/L_o$ as a function of time at 276 bar for PVDF homopolymer. With each increase of temperature, dilation increases with time, reaching a maximum value in about 1 hr. As the temperature increases from 127.2°C to 144.1°C, $\Delta L/L_o$ increases by 11.2%. Further increase to 145.9°C, results in a decrease of $\Delta L/L_o$. This trend continues till 149.2°C where a decrease in $\Delta L/L_o$ characteristic of melting is observed.

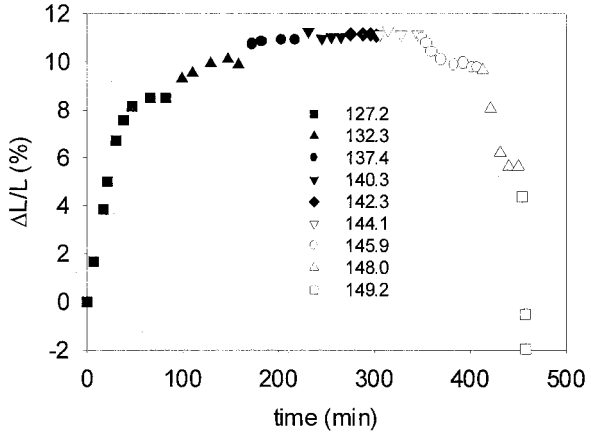

Fig. 1. $\Delta L/L_o$ for PVDF as a function of time at 276 bar from 127.2°C to 149.2°C.

Figure 2 shows a plot of PVDF dilation as a function of temperature in N_2 at ambient pressure and in supercritical CO_2 at 276, 476, 674 bar. At ambient pressure, the decrease in linear swelling occurs between 157°C and 159°C. We have designated T_m as the temperature halfway between the temperature of maximum swelling and the temperature at which the first loss of linear dimension occurs. Using this convention, LVDT measured T_m is 158°C. Alternatively, T_m may be described as the temperature at which $d(\Delta L/L_o)/dT$ becomes negative. This corresponds well to the maximum in the DSC melting endotherm (158°C).

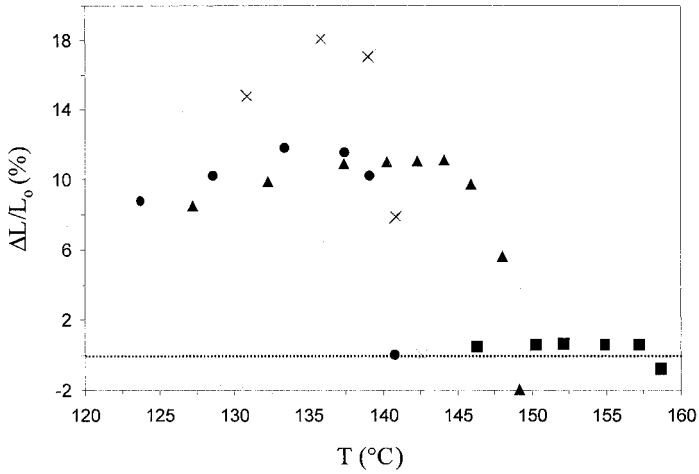

Fig. 2. Dilation of PVDF homopolymer as a function of temperature in nitrogen (N_2) at ambient pressure (■) and in supercritical CO_2 at 276 (▲), 476 (●), and 674 (x) bar.

In supercritical CO_2, initial dilation increases with temperature for all pressures (276, 476 and 674 bar) indicating homopolymer plasticization. The maximum for $\Delta L/L_o$ is ≈18% at 674 bar and 136°C. The temperature at which $d(\Delta L/L_o)/dT$ becomes negative is a function of the supercritical CO_2 pressure. The melting temperature, T_m decreases from 158°C at ambient pressure to ≈ 136°C in supercritical CO_2 at 476 bar, a decrease of 23°C. Further increase in CO_2 pressure results in a small increase in T_m to 137°C.

Figure 3 compares $\Delta L/L_o$ in nitrogen (N_2) at 276, 476, 674 bar with the dilation at ambient pressure. At lower temperatures, PVDF undergoes compression due to hydrostatic pressure effects. This is in contrast to the linear dilation in supercritical CO_2. Above 145°C, N_2 plasticization is minimal but a function of temperature with a 2.5% maximum dilation at 674 bar. In addition, $d(\Delta L/L_o)/dT$ becomes negative at temperatures greater than 158°C

indicating a slight increase in T_m with N_2 pressure. At 476 bar, T_m increases to 170°C and at 674 bar T_m increases to 173°C, an increase of 15°C.

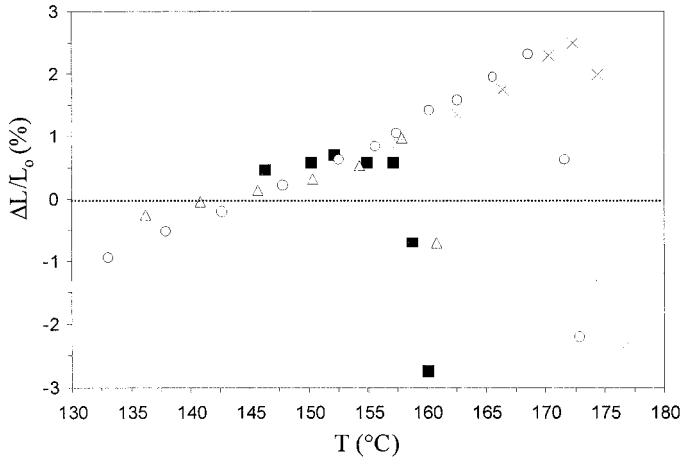

Fig. 3. $\Delta L/L_o$ of PVDF homopolymer as a function of temperature in nitrogen (N_2) at ambient pressure (■), 276 (Δ), 476 (O), and 674 (x) bar respectively.

The melting point of a polymer in high-pressure gas is a balance between plasticization due to polymer-gas interactions and hydrostatic pressure of the gas. The lowering of PVDF T_m in supercritical CO_2 is a result of reduction in the chemical potential of the amorphous phase due to favorable interactions between the CO_2-philic F and carbon dioxide[28]. Thus as pressure increases, T_m decreases to a minimum of 136°C at 476 bar due to increased CO_2 plasticization. However at 674 bar, our experimental limit, T_m increases to 137°C. At higher pressures, the decrease in T_m due to plasticization is offset by a modest increase in T_m due to higher hydrostatic pressure corresponding. Previously it has been documented that PVDF T_m increases ≈1°C for a 31 bar increase in hydrostatic pressure.[29,30] Thus above 476 bar, hydrostatic pressure effects offsets plasticization resulting in a small increase in T_m. In contrast to supercritical CO_2, N_2 is a "noninteracting gas".[31] Nitrogen plasticization is almost an order of magnitude smaller and the increase in T_m primarily reflects the effect of hydrostatic pressure.

PVDF copolymer. Figure 4 shows $\Delta L/L_o$ as a function of temperature for PVDF copolymer in N_2 at ambient pressure and in supercritical CO_2 at 276, 552 and 640 bar. At ambient pressure, the LVDT T_m using our convention ($d(\Delta L/L_o)/dT$) = negative) is 132°C. Copolymer

plasticization is observed for all pressures (276, 476 and 674 bar) with a maximum of ≈18% at 552 bar and 104°C. Plasticization and melting point depression are different for the copolymer due to lower crystallinity from disorder introduced by bulky CF_3 groups ($\Delta H_{copolymer}$ = 32 J/g versus $\Delta H_{homopolymer}$ = 51 J/g).

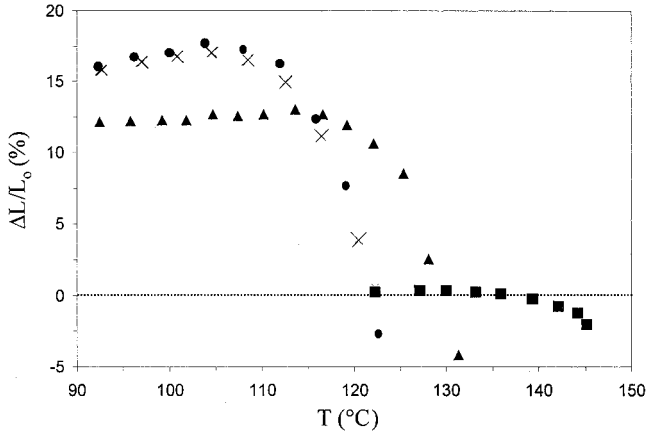

Fig. 4. PVDF copolymer dilation as a function of temperature in $SCCO_2$ in nitrogen (N_2) at ambient pressure (■) and in $SCCO_2$ at 276 (▲), 552 (●), and 640 (x) bar respectively.

For the copolymer, lowering of T_m in supercritical CO_2 is similar to the homopolymer. At 276 bar, T_m is ≈115°C, about 17°C lower than at ambient pressure (132°C). Increasing pressure to 552 bar, decreases copolymer T_m to 106°C, a decrease of 26°C. Further increase in pressure (640 bar) results in a small increase in T_m to 107°C. Though close to our experimental limits, it appears that PVDF-copolymer T_m is minimized at 552 bar. In summary, PVDF-copolymer plasticization (18%) is somewhat greater than homopolymer (14%) and T_m depression (27°C) is larger than PVDF homopolymer (23°C).

Figure 5 plots copolymer dilation in N_2 at 1, 276, 552, and 640 bar. At lower temperatures, N_2 plasticization is observed in contrast to the observed homopolymer compression. However, copolymer plasticization by N_2 is minimal (maximum $\Delta L/L_o$ = 1.3%) as expected. The LVDT measured T_m increases with increasing N_2 pressure. At 276 bar, copolymer T_m is 137°C an increase of 4°C. Copolymer T_m increases by 13°C at 552 bar and by 15°C at 630 bar.

A balance between plasticization and hydrostatic pressure determines copolymer T_m. At lower pressures (up to 552 bar) in supercritical CO_2 plasticization dominates (max $\Delta L/L_o$= 18%) and hence T_m decreases. At higher pressures, this decrease is offset by an increase in T_m due to

plasticization is observed for all pressures (276, 476 and 674 bar) with a maximum of ≈18% at 552 bar and 104°C. Plasticization and melting point depression are different for the copolymer due to lower crystallinity from disorder introduced by bulky CF_3 groups ($\Delta H_{copolymer}$ = 32 J/g versus $\Delta H_{homopolymer}$ = 51 J/g).

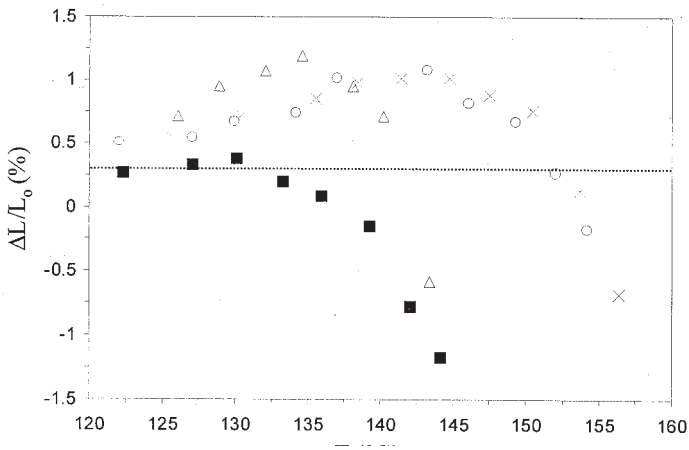

Fig. 4. PVDF copolymer dilation as a function of temperature in $SCCO_2$ in nitrogen (N_2) at ambient pressure (■) and in $SCCO_2$ at 276 (▲), 552 (●), and 640 (x) bar respectively.

For the copolymer, lowering of T_m in supercritical CO_2 is similar to the homopolymer. At 276 bar, T_m is ≈115°C, about 17°C lower than at ambient pressure (132°C). Increasing pressure to 552 bar, decreases copolymer T_m to 106°C, a decrease of 26°C. Further increase in pressure (640 bar) results in a small increase in T_m to 107°C. Though close to our experimental limits, it appears that PVDF-copolymer T_m is minimized at 552 bar. In summary, PVDF-copolymer plasticization (18%) is somewhat greater than homopolymer (14%) and T_m depression (27°C) is larger than PVDF homopolymer (23°C).

Figure 5 plots copolymer dilation in N_2 at 1, 276, 552, and 640 bar. At lower temperatures, N_2 plasticization is observed in contrast to the observed homopolymer compression. However, copolymer plasticization by N_2 is minimal (maximum $\Delta L/L_o$ = 1.3%) as expected. The LVDT measured T_m increases with increasing N_2 pressure. At 276 bar, copolymer T_m is 137°C an increase of 4°C. Copolymer T_m increases by 13°C at 552 bar and by 15°C at 630 bar.

A balance between plasticization and hydrostatic pressure determines copolymer T_m. At lower pressures (up to 552 bar) in supercritical CO_2 plasticization dominates (max $\Delta L/L_o$= 18%) and hence T_m decreases. At higher pressures, this decrease is offset by an increase in T_m due to

Acknowledgments

Financial support from Daikin Institute of Advanced Chemistry and Technology (DAI-ACT) and from the VCU School of Engineering Foundation is gratefully acknowledged.

[1] R. G. Wissinger; M. E. Paulaitis *J. Polym. Sci., Part B: Polymer Physics* **1987**, 25, 2497.
[2] B. J. Briscoe, Lorge, O., Wajs, A., Dang, P. *J. Polym. Sci., Part B: Polymer Physics* **1998**, 36, 2435.
[3] J. S. Wang; Y. Kamiya; Y. Naito *J. Polym. Sci., Part B: Polymer Physics* **1998**, 36, 1695-1702.
[4] Y. M. Kamiya, Keishin; Terada, Katsuhiko; Fujiwara, Yukihiko; Wang, Jin-Sheng. *Macromolecules* **1998**, 31, 472.
[5] *High Pressure Solid Polymer-Supercritical Fluid Phase behvaior*; I. S. M. Liau, M. A., Ed.; Elsevier Science Publishers: Amsterdam, netherlands, 1985.
[6] Y. G. Zhang, K. K.; Lemert, R. M. *J. Supercritical Fluids* **1997**, 11, 115.
[7] J. S. Chiou; J. W. Barlow; D. R. Paul *J. Appl. Polym. Sci.* **1985**, 30, 2633.
[8] P. D. J. Condo, K. P. *J. Polym. Sci., Part B: Polym. Phys.* **1994**, 32, 523.
[9] Y. P. Handa; P. Kruus; M. Oneill *J. Polym. Sci., Part B: Polymer Physics* **1996**, 34, 2635-2639.
[10] Z. K. Zhong; S. X. Zheng; Y. L. Mi *Polymer* **1999**, 40, 3829-3834.
[11] W. V. Wang; E. Kramer; W. H. Sachse *J. Polym. Sci., Part B: Polymer Physics* **1982**, 20, 1371.
[12] J. R. Royer; J. M. DeSimone; S. A. Khan *Macromolecules* **1999**, 32, 8965-8973.
[13] J. S. Chiou; J. W. Barlow; D. R. Paul *J. Appl. Polym. Sci.* **1985**, 30, 3911.
[14] S. M. R. Gross, G. W.; Kiserow, D. J.; DeSimone, J. M. *Macromolecules* **1999**, 32, 8965.
[15] W. J. P. Koros, D. R. *J. Poly. Sci.: Part-B: Polymer Physics* **1978**, 16, 1947.
[16] K. H. Mizoguchi, Takuji; Naito, Yasutoshi; Kamiya, Yoshinori. *Polymer* **1987**, 28, 1298.
[17] Y. T. Shieh; J. H. Su; G. Manivannan; P. H. C. Lee; S. P. Sawan; W. D. Spall *J. Appl. Polym. Sci.* **1996**, 59, 707-717.
[18] B. J. Briscoe; C. T. Kelly *Polymer* **1995**, 36, 3099-3102.
[19] B. J. Briscoe; S. Zakaria *J. Polym. Sci., Part B: Polymer Physics* **1991**, 29, 989.
[20] Y. P. Handa; J. Roovers; F. Wang *Macromolecules* **1994**, 27, 5511.
[21] Y. P. Handa; Z. Y. Zhang; J. Roovers *J. Polym. Sci., Part B: Polymer Physics* **2001**, 39, 1505-1512.
[22] K. Hatada; T. Kitayama; K. Ute; N. Fujimoto; N. Miyatake *Macromol. Symp.* **1994**, 84, 113-126.
[23] M. A. Singh; R. Hutanu; M. Shea; R. Fraser; T. Plivelic; Y. P. Handa *J. Polym.Sci., Part B: Polymer Physics* **2000**, 38, 2457-2467.
[24] Y. L. Mi; S. X. Zheng *Polymer* **1998**, 39, 3709-3712.
[25] Shenoy. S.; D. Woerdeman; R. Sebra; A. Garach-Domech; K. J. Wynne *Macromol. Rapid Commun.* **2002**, *23*, 1130-1133.
[26] S. L. Shenoy; T. Fujiwara; K. J. Wynne *Macromolecules* **2003**, accepted for publication.
[27] Z. Zhang; Y. P. Handa *Macromolecules* **1997**, 30, 8505.
[28] S. G. V. Kazarian, M. F.; Bright, F. V.; Liotta, C. L.; Eckert, C. A. *J. Am. Chem. Soc.* **1996**, 118, 1729.
[29] T. H. Hattori, M.; Ohigashi, H. *Polymer* **1996**, 37, 85.
[30] N. Mekhilef *J. Appl. Polym. Sci.* **2001**, 80, 230-241.
[31] M. Mulder *Basic Principles of Membrane Technology*; Second ed.; Kluwer Academic Publishers, Boston, 1997.